ELSEVIER

Earth and Planetary Science Letters 210 (2003) 333–349

EPSL

www.elsevier.com/locate/epsl

# Composition of the Uralide crust from seismic velocity ($V_p$, $V_s$), heat flow, gravity, and magnetic data

D. Brown [a,*], R. Carbonell [a], I. Kukkonen [b], C. Ayala [a], I. Golovanova [c]

[a] *Instituto de Ciencias de la Tierra 'Jaume Almera', c/Lluis Sole i Sabaris, s/n, 08028 Barcelona, Spain*
[b] *Geological Survey of Finland, Betonimiehenkuja 4, P.O. Box 96, FIN-02151 Espoo, Finland*
[c] *Ufimian Geoscience Centre, Russian Academy of Science, 16/2 K. Marx, Ufa 450000, Russia*

Received 15 November 2002; received in revised form 7 March 2003; accepted 7 March 2003

**Abstract**

P-wave velocity ($V_p$), S-wave velocity ($V_s$), Poisson's ratio ($\sigma$), heat flow, potential field, and surface geological data are integrated to constrain a model for the composition of the Uralide crust along the URSEIS transect. The model is constructed using published laboratory measurements of $V_p$, $V_s$, $\sigma$ and density for a variety of crustal rock types. These laboratory data have been corrected for depth (pressure) and the Uralides temperature–depth function. The model shows clear differences between the composition of the old continental crustal nucleus of the East European Craton and the newly added crust of the accreted arc terranes to the east. The crust of the East European Craton is more felsic than that of the Magnitogorsk and East Uralian zones, and the latter two have a lowermost crust whose characteristics indicate a high garnet content (mafic garnet granulite) and/or the presence of hornblendite. The overall composition of the arc terranes is basaltic. Physical properties suggest that eclogite is not present in the arc terranes, or if present it exists in small amounts that are below the resolution of the data set. The lack of eclogite in the lower crust favours an intracrustal differentiation model for the evolution of the bulk composition of the continental crust. Nevertheless, the absence of surface uplift, the lack of metamorphism and late orogenic mantle melts, and the current crustal thickness indicate that crustal thinning did not affect the bulk composition of the Uralide crust.


*Keywords:* Uralides; petrophysical model; crustal composition

## 1. Introduction

The composition of the continental crust has long been a subject of interest to Earth scientists since it provides key information about the growth and evolution of the continents. One of the main ways in which continents are thought to grow is by the accretion of volcanic arcs (new crust) to a continental margin (old nucleus) along subduction zones (see Rudnick [1] for an overview). It has been suggested recently [2,3] that this process resulted in an important phase of crustal growth during the Palaeozoic, in the Altaid collage of what was then the evolving Pangaea, when vast volcanic arc complexes added an estimated ~5.3 million km$^2$ of new crust to the continent [2]. This process of arc–continent colli-

* Corresponding author. Tel.: +34-93-409-54-10; Fax: +34-93-411-00-12.
*E-mail address:* dbrown@ija.csic.es (D. Brown).

0012-821X/03/$ – see front matter 
doi:10.1016/S0012-821X(03)00143-2

sion in the Altaid collage has been particularly well studied in the Uralide orogen of central Russia [4–7]. The Uralides grew as intraoceanic island arcs that had developed in the palaeo-Uralian ocean, accreted to the margin of the East European Craton [4–7]. Concomitantly, Andean-type arcs are thought to have formed on the other side of the Uralian ocean, on the margin of the Siberian plate [8]. With the closure of the Uralian ocean basin and cessation of the Uralide orogeny in the Late Palaeozoic these arcs had added approximately 200 million km$^3$ of new crust (assuming a current average Uralide crustal thickness of 40 km) to Pangaea. With the exception of minor Triassic transtension, intraplate volcanism, and basin inversion during the development of the West Siberian Basin, the Uralide orogen has been preserved, relatively intact, since the Permian, providing an ideal place to study the composition of the continental crust and to test a model for its growth and evolution since the Palaeozoic. This is particularly the case in the southern Uralides (Fig. 1), where the development of the West Siberian Basin had almost no effect and intraplate volcanism was not manifested.

In this paper we present surface geology, reflection seismic, P-wave velocity ($V_p$), S-wave velocity ($V_s$), heat flow, gravity, and magnetic data along the Urals Seismic Experiment and Integrated Studies (URSEIS) transect in the southern Uralides (Fig. 1) from which a model of the crustal composition is constructed. Although such modeling is non-unique, the seismic velocities ($V_p$, $V_s$, as well as Poisson's ratio or $V_p/V_s$), density, and heat production can be reasonably well correlated with laboratory measurements of these parameters on average crustal rock types, and have provided an important data set for determining crustal composition [9–11]. A complication that arises in this model is that surface occurrences of lower crustal rocks are restricted to xenoliths in granitoids, which are predominantly mafic in composition, and to high-grade metamorphic terranes that are predominantly felsic to intermediate in composition [11–15], making it difficult to assess these two different lithologies with respect to the composition of the deep crust [1,11,16]. Furthermore, the andesitic model for continental crustal composition contains a dilemma: the volcanic arcs from which continental crustal is thought to have formed have a basaltic bulk composition [1,17]. A proposed solution to this dilemma is that arc crust must undergo intracrustal differentiation, perhaps by metamorphic reactions, following accretion to form intermediate to felsic melts that rise through the crust and an ultramafic (eclogitic) restite that remains in the lower crust [18–20]. In this model, the dense ultramafic crust then delaminates and sinks into the mantle, leaving behind an andesitic continental crust. An obvious corollary to this process is that the continental crust is thinned, with resultant uplift at the surface and invasion of hot mantle material at the base of and into the crust. Can such a model be applied to the thick (50–60 km) Uralide crust, whose mostly very low-grade metamorphism suggests little surface uplift and erosion and whose late orogenic granitoids show little evidence of a mantle contribution (see below)?

## 2. The southern Urals

### 2.1. Surface geology

The south Urals foreland thrust and fold belt (Fig. 1) consists of a west-vergent, basement-involved, thrust system overlain by a stack of allochthons belonging to an arc–continent collision accretionary complex [5,21–23]. The stratigraphy of the foreland thrust and fold belt consists of Archaean to Early Proterozoic intermediate to mafic gneiss overlain by up to 12 000 m of Proterozoic clastic sediments, with lesser amounts of limestone, and volcanic and subvolcanic rocks locally [24]. To the east of the Zuratkul fault (Fig. 1) the Proterozoic sediments are polydeformed and metamorphosed up to upper amphibolite facies. The Palaeozoic platform sediments consist of approximately 3000 m of unmetamorphosed carbonates with minor clastics [4]. The Upper Carboniferous to Lower Triassic foreland basin consists of more than 3000 m of westward-thinning bioclastic sediments, marls, limestone, and evaporites, locally overlain by conglomerate and sandstone [25]. The accretionary complex (Fig. 1) is

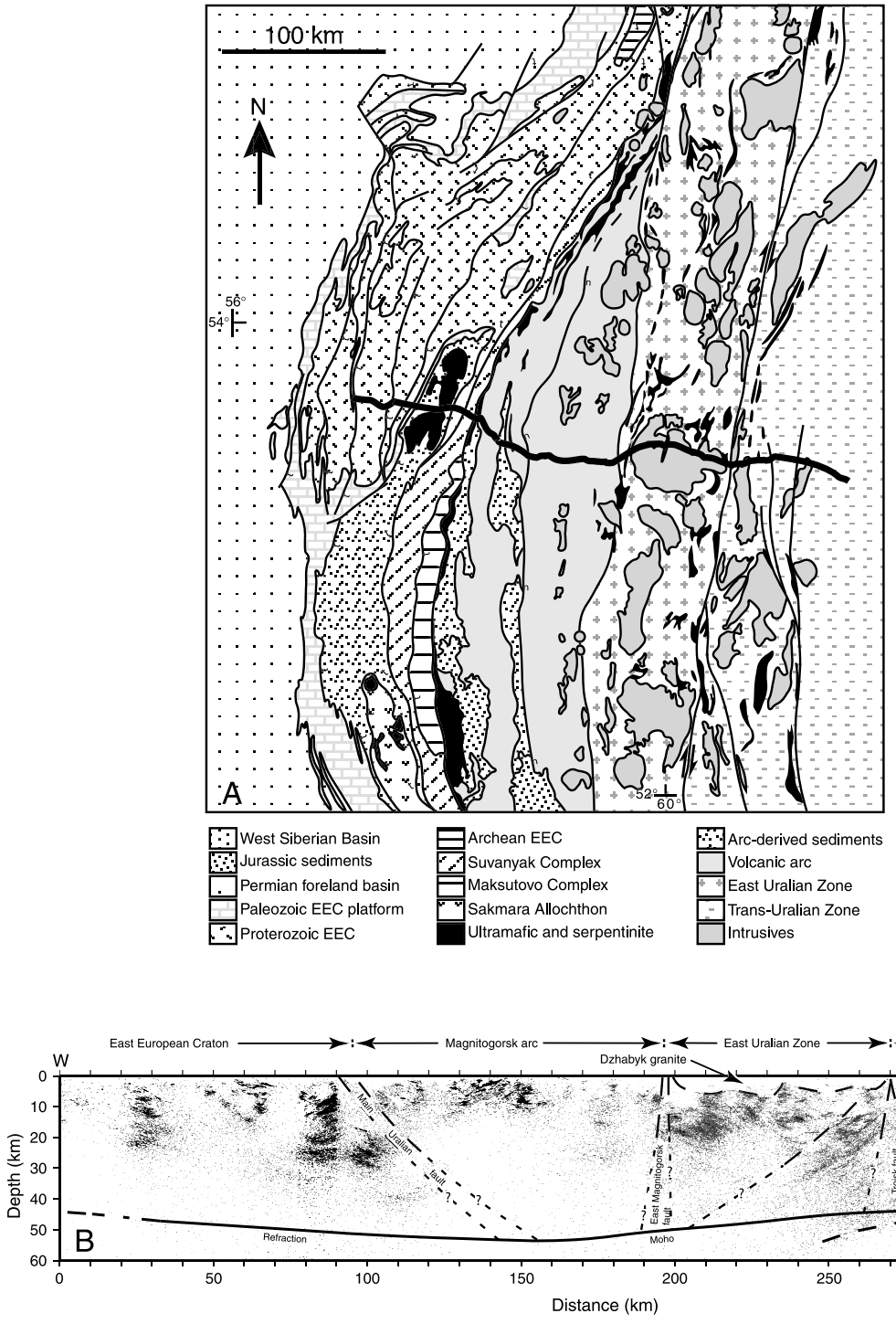


Fig. 1. (A) Geological map of the southern Urals showing the location of the URSEIS transect. (B) Line drawing of the URSEIS vibroseis data [30] for the portion of the transect covered by the wide-angle data. Note that the scale of the seismic profile is not that of the map.

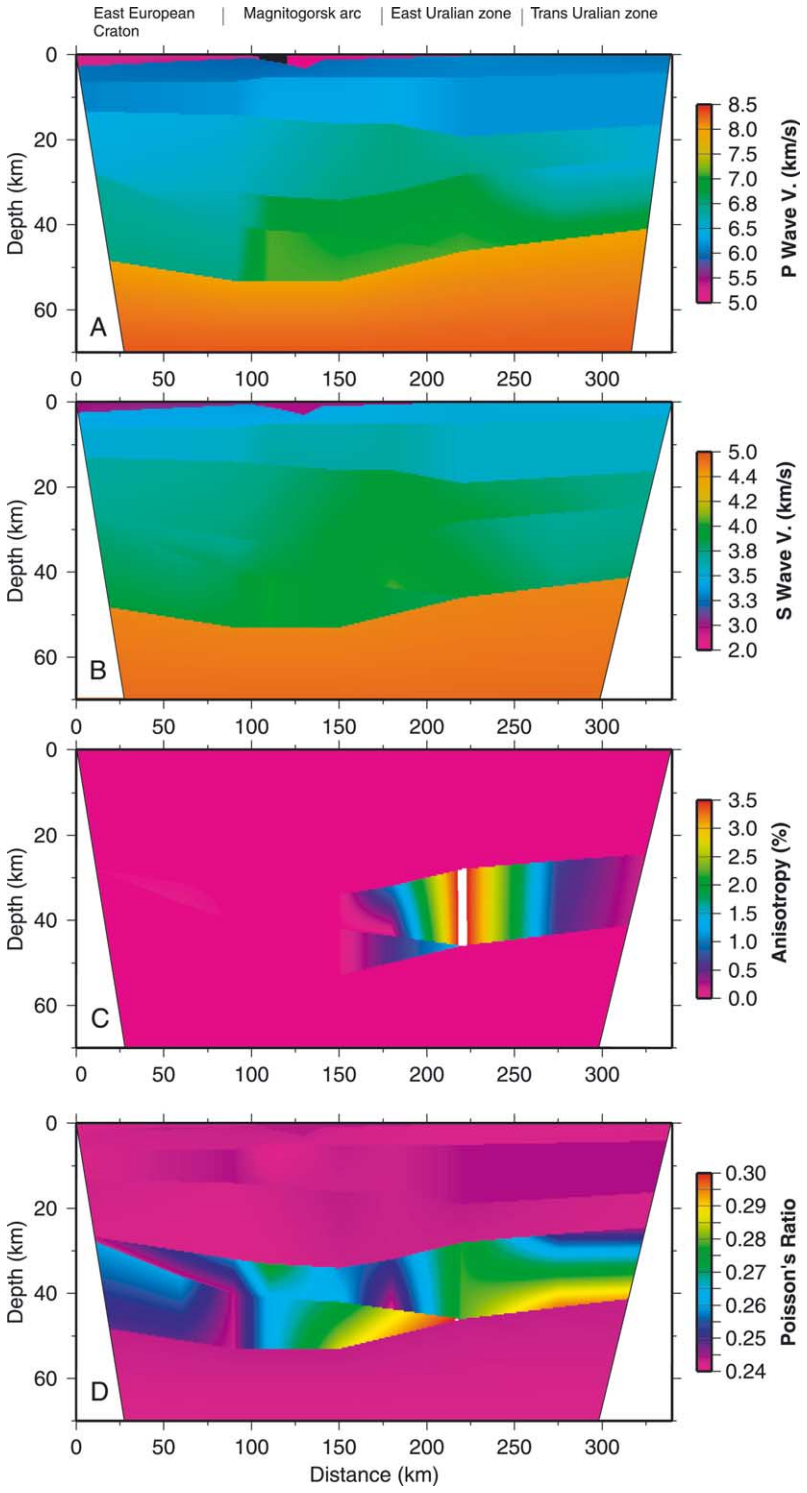
East European Craton
Magnitogorsk arc
East Uralian zone
Trans Uralian zone
Depth (km)
Distance (km)
A
B
C
D
P Wave V. (km/s)
S Wave V. (km/s)
Anisotropy (%)
Poisson's Ratio

composed of weakly metamorphosed metasediments (Suvanyak Complex) that are overthrust by ~5 km of late Frasnian and Famennian volcaniclastic turbidites (Zilair Formation) [5,26]. Along the URSEIS profile, these units are structurally overlain by the Kraka lherzolite massif. The East European craton is sutured to the Magnitogorsk arc along the Main Uralian fault, a wide melange zone.

The Silurian to Late Devonian Magnitogorsk island arc is comprised of boninite-bearing arc tholeiites and calc-alkaline volcanics [6]. In the west, these volcanic units are overlain by up to 5000 m of clastic sediments [27,28]. Lower Carboniferous limestone and minor clastics unconformably overlie the arc edifice and, locally, Lower Carboniferous granitoids intrude into it. Deformation in the Magnitogorsk arc is small, with only minor, open folds and minor thrusting [28]. The metamorphic grade is very low, barely exceeding seafloor metamorphism. To the east, the arc is structurally juxtaposed against the East Uralian zone along the East Magnitogorsk fault zone.

The East Uralian zone crossed by the URSEIS transect is composed of deformed greenschist to amphibolite facies schist and gneiss. The East Uralian zone has been extensively intruded by Late Carboniferous and Permian granitoids (Fig. 1). In the area crossed by the URSEIS transect the East Uralian zone is bounded to the east by a several kilometres wide melange that contains relics of harzburgite locally. This boundary forms a prominent NNE-striking aeromagnetic lineament (see below).

The Trans-Uralian zone is not well known owing to its poor exposure. What is known suggests that it is composed of variably metamorphosed, tectonically imbricated Palaeozoic volcanic arc fragments and Precambrian and Palaeozoic sediments interpreted to be of continental origin [29]. The best known units are Devonian and Carboniferous calc-alkaline volcano-plutonic complexes composed predominantly of volcaniclastics and lava flows [4]. Ophiolite units and high-pressure rocks have also been reported [4]. The volcanic sequences are intruded by comagmatic gabbro–diorite and diorite plutons. The volcano-plutonic complexes are overlain by terrigenous red beds and evaporites. The deformation has not been well studied, although it appears that the Devonian and Lower Carboniferous units are affected by open to tight folds and east-vergent thrusting.

## 3. Geophysical data

### 3.1. Reflection data (crustal architecture)

The URSEIS vibroseis deep reflection seismic data show the southern Uralide crust to be composed of four major blocks with distinctive reflection characteristics juxtaposed along crustal-scale boundaries [30,31] (Fig. 1). The foreland thrust and fold belt is imaged as subhorizontal to east-dipping reflectivity that can be related to its Palaeozoic and older tectonic history. The Moho beneath the foreland thrust and fold belt is not imaged in the vibroseis data set, although explosion source reflection data [32] and wide angle data [33] show it to deepen eastward from approximately 42 km to nearly 53 km (Fig. 1). The Main Uralian fault (the major arc-continent suture) is unreflective, but its subsurface location can be inferred by the truncation of the reflection pattern of the East European craton and its contrast with that of the Magnitogorsk arc. The Magnitogorsk arc reflectivity is characterised by patchy reflections in the upper ~10–15 km. Below this, reflectivity is diffuse, or the arc crust is transparent, and the Moho is not imaged. The East Magnitogorsk fault zone, which juxtaposes the arc against the East Uralian zone, is not imaged by the data, although truncation of East

←

Fig. 2. (A) $V_p$ model of the Uralide crust along the URSEIS transect. (B) $V_s$ model of the Uralide crust. The model was calculated using the average of the N–S and E–W horizontal components of the shear wave velocity. (C) Anisotropy model of the Uralide crust. Uncertainties on the calculated anisotropy are ±0.5%. (D) Poisson's ratio model of the Uralide crust. Uncertainties on the Poisson's ratio are ±0.01.

Uralian zone reflectivity suggests its presence in the subsurface [30]. The upper 5–6 km of the East Uralian zone, corresponding to the Dzhabyk granite, is transparent. Below the granite the crust is characterised by east-dipping patches of reflections that in the east become shallowly west-dipping. A ~10 km thick, west-dipping band of reflections between 12 and 35 km depth, the Kartaly Reflection Sequence, extends beneath almost the entire East Uralian zone. The crust beneath the easternmost East Uralian zone reaches 53 km in thickness. The upper and middle crust of the Trans-Uralian zone is characterised by a series of east- and west-dipping, concave-upward reflections. The lowermost middle and lower crust displays thin bands of west-dipping reflectivity. The Moho is imaged as a sharp transition from reflective lower crust to transparent upper mantle at ~49 km depth, and the lower crustal reflections appear to merge with it.

### 3.2. Velocity data

The crustal velocities described here (Fig. 2) are taken from the wide-angle data of Carbonell et al. [34] and the reader is referred there for details of acquisition, processing and generation of the velocity models. The upper crust along the URSEIS transect is characterised by P-wave velocities ($V_p$) of up to 6.2 km/s to a depth of approximately 13 km in the East European Craton and Magnitogorsk arc (Fig. 2A). Eastward, in the East and Trans-Uralian zones, the upper crustal $V_p$ reaches 6.2–6.3 km/s to a depth of between 15 and 18 km. Below these depths there is a gradual increase in $V_p$ to values of up to 6.7 km/s. In the westernmost part of the East European Craton there is a jump in $V_p$ from 6.5 to 6.7 km/s at about 25–30 km depth that disappears eastward. From the Main Uralian fault eastward there is a velocity jump from 6.4 km/s at the base of the upper crust to between 6.6 and 6.8 km/s at the top of the middle crust and then a gradual increase to up to 7.0 km/s above the Moho. $V_p$ in this area also increases eastward to a maximum in the eastern part of the Magnitogorsk arc and the western part of the East Uralian zone, after which it decreases again. The lowermost crust to the east of the Main Uralian fault is characterised by an eastward-thinning band of $V_p$ of 7.0–7.1 km/s. The crust–mantle boundary is marked by an increase in $V_p$ to $>8.0$ km/s. The average Uralide $V_p$ versus depth function closely matches that of the average continental crust [10] (Fig. 3).

The $V_s$ model shown in Fig. 2B is an average of the north–south and the east–west components of the S-wave velocity models [34]. Since S-wave anisotropy is weak throughout most of the Uralide crust (Fig. 2C), with values of 2–3% being reached only in a several kilometres thick band overlapping the Kartaly Reflection Sequence in the East and Trans-Uralian zones, the model in Fig. 2B provides a reasonable approximation to the $V_s$ structure of the Uralides and is suitable for deter-

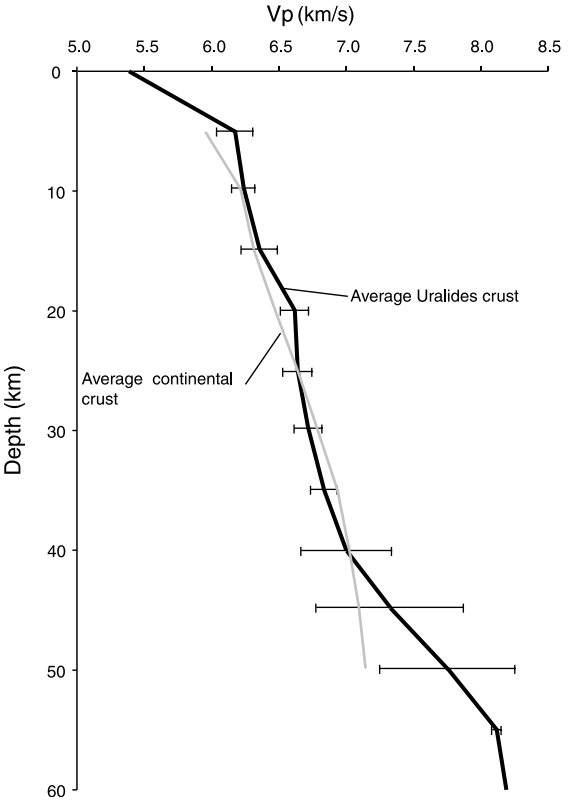


Fig. 3. Velocity–depth functions for the average continental crust [10] and for the average Uralide crust are closely matched. However, the velocity–depth function changes significantly from one unit to another across the Uralides. Horizontal lines on the Uralides curve indicate one standard deviation.

mining Poisson's ratio. The upper crustal S-wave velocities ($V_s$) in the East European Craton reach 3.5–3.6 km/s at a depth of about 13 km, increasing in the Magnitogorsk arc to 3.9 km/s, and decreasing again to a maximum of 3.6 km/s at about 15–17 km depth in the East and Trans-Uralian zones. Below this there is a jump in $V_s$ to between 3.7 and 3.9 km/s and then a gradual increase to between 3.9 and 4.0 km/s at the Moho. $V_s$ in the middle and lower crust increases eastward to a maximum in the eastern part of the Magnitogorsk arc and the western part of the East Uralian zone, after which it decreases again. The lowermost crust in the eastern part of the Magnitogorsk arc and the western part of the East Uralian zone is marked by a high-$V_s$ zone in which velocities reach 3.9–4.0 km/s. The crust–mantle boundary is characterised by an increase from crustal velocities of $\leq 4.0$ km/s to mantle velocities of $> 4.6$ km/s.

The crust along the URSEIS transect is characterised by a uniform $\sigma$ of 0.25 to a depth of about 25 km in the west and east, increasing in depth to 33 km in the central part of the Magnitogorsk arc. In the East European Craton there is an eastward-dipping increase in $\sigma$ from 0.25 to 0.26, which characterises the lower crust. Beneath the Magnitogorsk arc and the East Uralian zone $\sigma$ values jump from 0.25 to 0.27, although this jump is not found in the Trans-Uralian zone. The lowermost crust beneath the Magnitogorsk arc and the East and Trans-Uralian zones is marked by $\sigma$ values of 0.28–0.29. Poisson's ratio ($\sigma$) provides an important constraint on the estimation of crustal composition since it can be related to the $SiO_2$ content [9]. However, $\sigma$ analysis is hampered by the fact that most common rock types fall within a narrow range (0.21–0.31) with a calculated uncertainty of $\pm 0.01$ [35].

### 3.3. Heat flow data

The Uralides heat flow density (HFD) has a strong minimum along the central axis of the orogen (Fig. 4). The low (10 mW/m$^2$) and the short wavelength of the anomaly are suggestive of a shallow origin for the minimum. The heat production (HP) data indicate that surface samples have HP values of 0.5 mW/m$^2$ on average (arithmetic average even as high as 0.8 mW/m$^2$ [36]), which is too much to allow a HFD minimum to be simulated by the model. This implies that there could be more ultramafic material at depth beneath the Magnitogorsk zone than below the East European Craton (see below). Another possibility is that the HFD minimum does not exist, and the anomaly might be attributed to palaeoclimatic disturbances [36]. Palaeoclimatic disturbances on the geothermal gradient decrease with increasing depth. Since measurements from boreholes in the area of the HFD low are shallower than in the surrounding areas, palaeoclimate may influence these values more. In the present modelling, the first alternative is followed.

The thermal conductive model of the URSEIS profile was constructed and calculated with a finite difference steady-state heat transfer code. Thermal conductivity was assumed to be temperature-dependent [36]. The model is 2-D, 450 km long and 200 km deep. Only the part corresponding to the velocity model (Fig. 2) is shown in Fig. 4. Discretisation was 1–5 km in the vertical and 10 km in the horizontal dimension. Heat flow data are from Kukkonen et al. [36] and references therein. Heat production data were adapted from the analyses and compiled literature data [36]. Additional constraints were placed on the model using mantle xenolith $P$–$T$ data from the Siberian craton to estimate mantle heat production [36]. In the model, a mantle HFD value of 13 mW/m$^2$ at 200 km was used. Thus, the lithosphere/asthenosphere boundary is not explicitly included in the model.

Although the model is dependent on the applied heat production values, and contains naturally inherent uncertainty, the results do not suggest a very cold root under the central axis of the Uralides (see below). This is interpreted to be the result of crustal thickening increasing the total heat production (crustal rocks produce more heat than mantle rocks), and the fact that the Magnitogorsk arc rocks cannot have a completely negligible heat production. Furthermore, the thermal conductivity of the crustal rocks is lower than that of the mantle, which increases the gradient (and temperatures) in the crust in comparison to

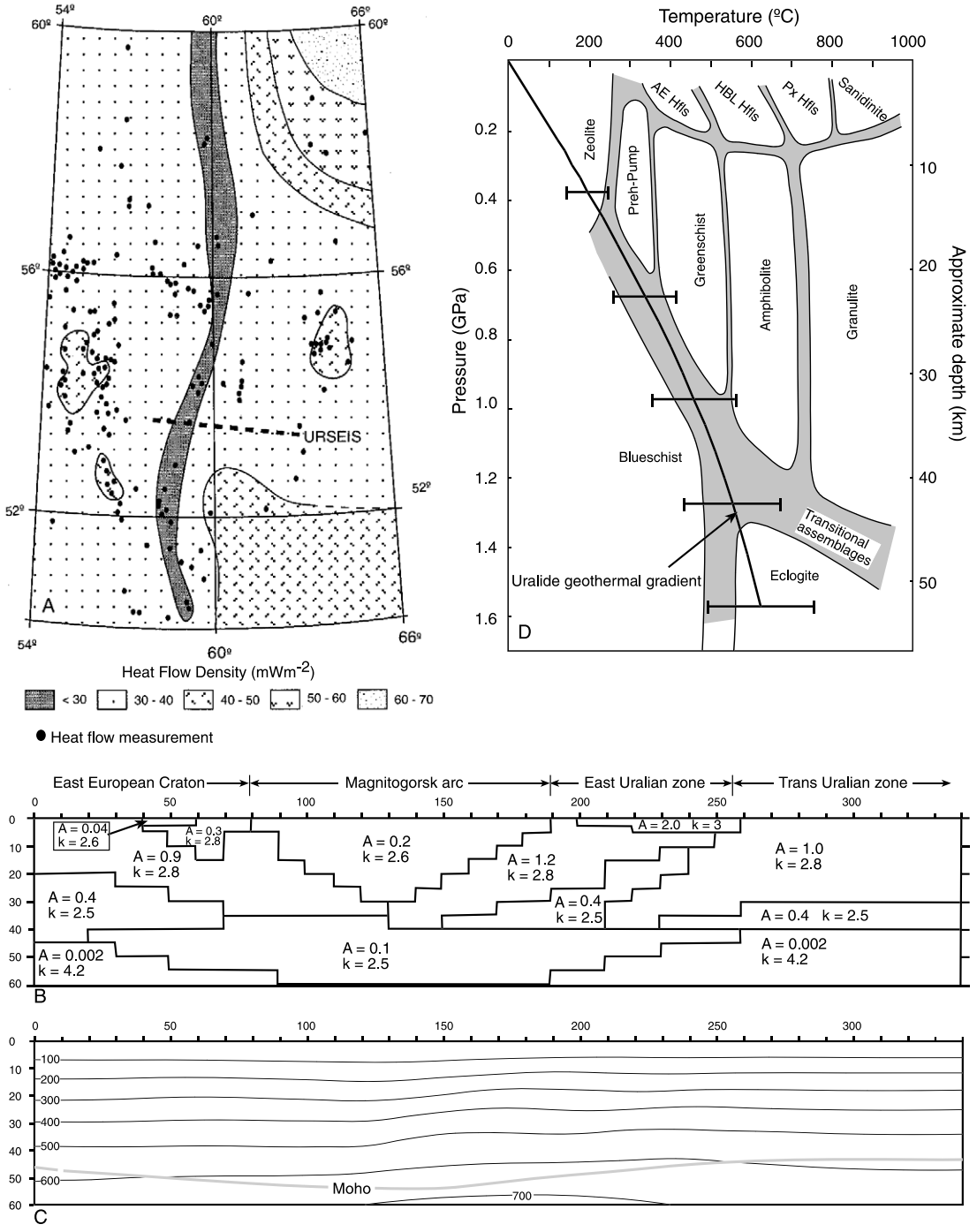


Fig. 4. (A) HFD map of the southern Uralides. Points indicate the location of data. (B) Heat production ($k$) and conductivity ($A$) model for the Uralides heat flow density data along the URSEIS transect (dashed line in A). (C) Geotherm model for the URSEIS transect. The grey line indicates the Moho determined from the URSEIS seismic data. (D) Uralides temperature–depth function plotted on a metamorphic facies map suggests that the Uralide crust is composed of mostly low metamorphic grade rocks. Horizontal lines on the curve indicate one standard deviation.

the mantle. However, the heat flow values show a minimum of about 10 mW/m$^2$ in the Magnitogorsk zone, satisfying the requirement of the HFD minimum. The HFD contrast is limited to the upper and middle crust, and no minimum is present in the lower crust and mantle beneath the Magnitogorsk zone.

In using the temperature data for lithological interpretation of the published laboratory seismic velocities that follows, it has been taken into account that considerable uncertainty is related to typical geothermal model results. Calculated temperatures at 50 km depth may be accurate to about ±100°C, as suggested by Monte Carlo simulations [37]. This is created by the uncertainties in the values of conductivity and heat production rate as well as the lower boundary conditions.

### 3.4. Gravity and magnetic data

A 2-D gravity and magnetic model along the URSEIS transect is shown in Fig. 5. The gravity field comes from Kimbell et al. [38]. The Bouguer anomaly profile is characterised by a low of between −60 and −45 mGal across the East European Craton that abruptly increases to between about 0 and –40 mGal across the Magnitogorsk zone. The East Uralian zone is characterised by a low of between about −70 and −40 mGal, increasing again to between about −30 and −10 mGal across the East Uralian zone. A starting density model was made by conversion of $V_p$ to density using the equation of Sobolov and Babyenko [40]. The East European Craton upper and middle crust are largely modelled (Fig. 5) with densities of about 2.8 and 2.9 g/cm$^3$ with small local variations to account for short-wavelength features. The lower crust is modelled with higher densities of 2.98 and 3.02 g/cm$^3$. To the east of the Main Uralian fault, much of the upper crust is modelled with densities of between 2.71 and 2.8 g/cm$^3$, although densities are somewhat higher in the Magnitogorsk zone. The middle crust (and part of the upper crust in the Magnitogorsk zone) is modelled with densities of between 2.92 and 2.95 g/cm$^3$. The lower crust is modelled with densities of between 2.98 and 3.07 g/cm$^3$. The upper mantle, at the depth shown, is modelled with a density of 3.34 g/cm$^3$.

The magnetic profile contains high-amplitude, short-wavelength features which tend to mask the longer-wavelength anomalies. However, there is a significant long-wavelength magnetic low centred over the orogen which has an amplitude of several hundred nT that reflects the magnetic character of the basement. The magnetic crystalline basement of the East European Craton at the west end of the profile is truncated at around 300 km, about 50 km to the west of the Main Uralian fault [39]. The eastward rise in the magnetic field on the eastern side of the profile is modelled by introducing magnetic basement east of the Kartaly Reflection Sequence (east of about 150 km). Magnetic susceptibilities throughout the East European Craton crust are modelled as 0 and 1.5 A/m to the east and west of the Zuratkul fault, respectively. Magnetic susceptibilities of the upper crust vary between 0.25 and 0.5 A/m, with areas reaching 2 and even 2.5 A/m locally. The middle and lower crust is modelled with magnetic susceptibilities of 0.5 and 1.5 A/m. Although alternative geometries are possible (assuming different magnetic structures for the basement), this model provides an acceptable fit to the observed anomalies [38,39].

## 4. Discussion

The crustal composition model discussed below was constructed by comparing the Uralide data set with the published $V_p$, $V_s$, Poisson's ratio and density data set [9,10]. P-wave velocities for each rock type have been corrected for depth and the Uralide geothermal gradient using published thermal coefficients [10]. $V_s$ was recovered from the corrected $V_p$ using the published Poisson's ratio [9] for each rock type (Table 1). $V_p$ versus $V_s$ for the various lithologies plot in a cluster around the Uralide values for the different levels in the crust (Fig. 6A), with the exception of mafic eclogite, which plots well outside the Uralide values. $V_p$ versus Poisson's ratio shows a wide scatter, especially for the basalt series and for mafic eclogite (Fig. 6B). The $V_p$ versus density (Fig. 6C)

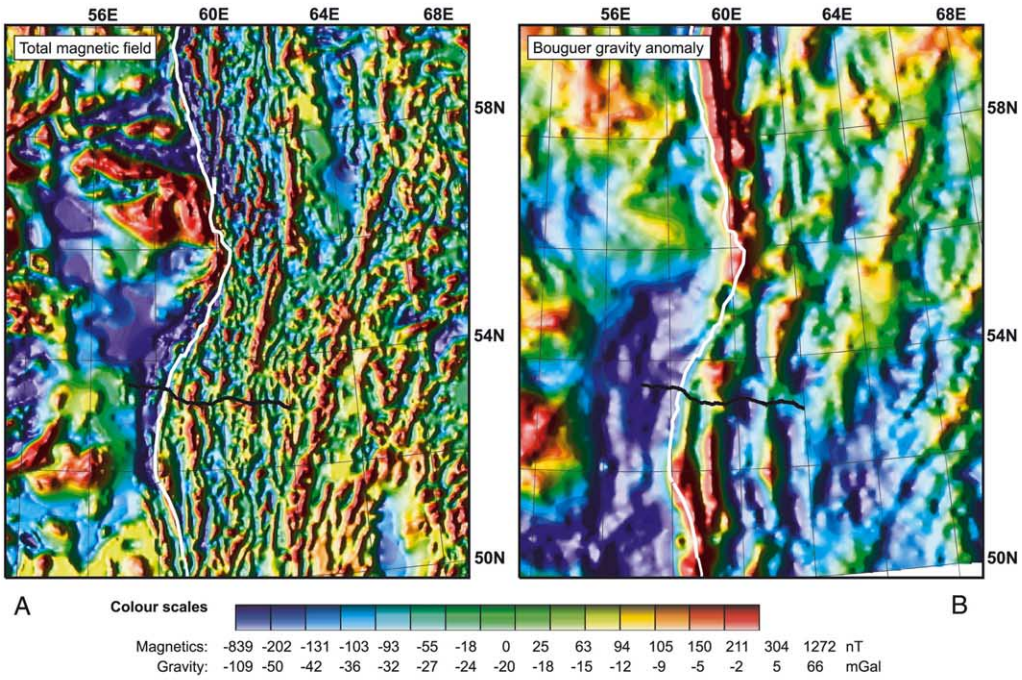
56E
60E
64E
68E
Total magnetic field
Bouguer gravity anomaly
58N
54N
50N
A
B
Colour scales
Magnetics: -839 -202 -131 -103 -93 -55 -18 0 25 63 94 105 150 211 304 1272 nT
Gravity: -109 -50 -42 -36 -32 -27 -24 -20 -18 -15 -12 -9 -5 -2 5 66 mGal

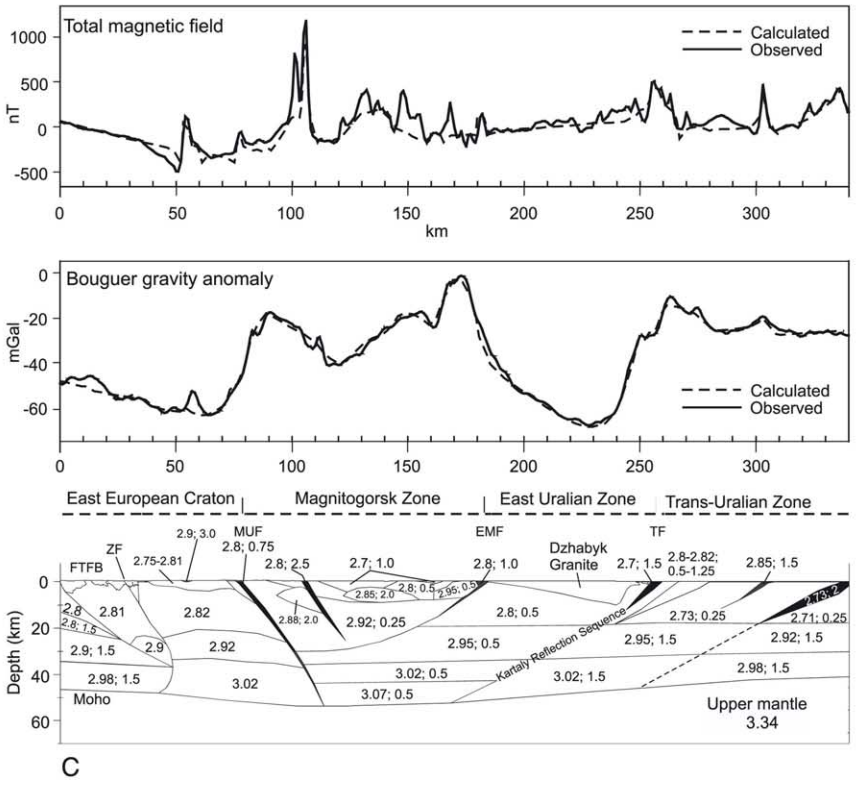
Total magnetic field
Calculated
Observed
nT
km
Bouguer gravity anomaly
mGal
East European Craton
Magnitogorsk Zone
East Uralian Zone
Trans-Uralian Zone
FTFB
ZF
MUF
EMF
TF
Dzhabyk Granite
Kartaly Reflection Sequence
Moho
Upper mantle
3.34
Depth (km)
C

plot has a cluster around the Uralides values, although mafic eclogite again plots well outside this cluster. Based on these analyses, a best estimate model of the Uralide crustal composition is shown in Fig. 7A. In Fig. 7B a geological interpretation has been added to the model using constraints provided by surface geology and the crustal architecture derived from the reflection seismic data (Fig. 1). The models presented in Fig. 7A,B suggest a significant difference between the composition of the East European Craton crust and that of the accreted crust to the east, in particular in the nature of the lowermost crust.

The low velocities in the upper 5 km of the western half of the profile are likely the result of cracks and fluid, and therefore cannot be considered reliable for estimating composition. The average composition of the upper crust in the East European Craton is best characterised by phyllite and perhaps slate and mica quartz schist (Figs. 6 and 7). Granite and biotite gneiss both fall within the acceptable values (Fig. 6), but since neither fits the known geology of the foreland thrust and fold belt they are discarded. The velocity and density data for the East European Craton middle crust fall outside the values for most of the measured rock types, although the composition may be best characterised by mica quartz schist, felsic granulite and paragranulite. The East European Craton lower crust is likely composed of amphibolite and mafic granulite, which is in keeping with the lithology of the Archaean crystalline basement in outcrop. The East European Craton fits quite well with the generalised continental crustal model of an andesitic upper crust overlying a mafic lower crust. It has been suggested that eclogitised East European Craton lower crust makes up the root zone of the Uralides [41], but this is not supported by the data presented here (Fig. 6), or eclogite is present in amounts below the resolution of the analyses presented in this paper (e.g., [42]).

The subsurface geological interpretation of the Magnitogorsk arc is complicated by the complex lithologic, velocity and density structure commonly found in volcanic arcs [43–45]. The composition of the upper and part of the middle crust of the Magnitogorsk zone is not well constrained by the velocity and density data (Fig. 6), but on the basis of surface geology is interpreted to consist of zeolite to prehnite–pumpellyite facies basalt and its intrusive equivalents (diabase, diorite, and tonalite). The lower part of the middle crust fits the parameters for greenschist facies basalt, amphibolite, and mafic granulite quite well. The Magnitogorsk arc lower crust appears to be composed of gabbro–norite, mafic garnet granulite or hornblendite. An important point to note is that the composition of the Magnitogorsk arc can be characterised by its physical properties as basaltic or some derivative of it (e.g., diabase or mafic granulite). This is in keeping with the basaltic source determined for the Magnitogorsk volcanic suites on the basis of its geochemistry [46], and with the current understanding that island arcs are predominantly basaltic in composition [17]. It is also consistent with the basaltic origin for the late-orogenic small gabbro–granite plutons in the Magnitogorsk arc [8]. It is, however, in conflict with the andesitic bulk composition model commonly proposed for the continental crust [1], and is problematic with respect to the intracrustal differentiation model [18,19] (see below).

The upper and middle crust of the East Uralian and Trans-Uralian zones is best characterised by low metamorphic grade sediments, basalt, granite, and/or felsic gneiss (Fig. 6). The middle crust in the East Uralian zone, and extending into the lower crust in the Trans-Uralian zone, is best characterised by greenschist facies basalt, amphibolite, and mafic granulite (and to a lesser extent

←

Fig. 5. (A) Total magnetic field map and (B) Bouguer gravity map of the southern Uralides. (C) Density and magnetic model of the Uralide crust along the URSEIS transect. Numbers indicate density (Mg/m$^3$) and magnetisation (A/m). Zero magnetisation is assumed unless otherwise indicated. EMF = East Magnitogorsk fault; FB = foreland basin; FTFB = foreland thrust and fold belt; MUF = Main Uralian fault; TF = Troitsk fault; ZF = Zuratkul fault. The location of the model is shown in A and B by the black line. Redrawn from [38].

Table 1
$V_p$, $V_s$ and density of crustal rocks corrected for depth and average Uralide geothermal gradient

| | 5 km 70°C | | | 10 km 128°C | | | 15 km 222°C | | | 20 km 302°C | | | 25 km 370°C | | | 30 km 432°C | | | 35 km 485°C | | | 40 km 535°C | | | 45 km 572°C | | | 50 km 608°C | | |
|---|---|---|---|---|---|---|---|---|---|---|---|---|---|---|---|---|---|---|---|---|---|---|---|---|---|---|---|---|---|---|
| | $V_p$ | $V_s$ | $\rho$ | $V_p$ | $V_s$ | $\rho$ | $V_p$ | $V_s$ | $\rho$ | $V_p$ | $V_s$ | $\rho$ | $V_p$ | $V_s$ | $\rho$ | $V_p$ | $V_s$ | $\rho$ | $V_p$ | $V_s$ | $\rho$ | $V_p$ | $V_s$ | $\rho$ | $V_p$ | $V_s$ | $\rho$ | $V_p$ | $V_s$ | $\rho$ |
| Andesite | 5.39 | 2.91 | 2.57 | 5.55 | 3.00 | 2.59 | 5.60 | 3.02 | 2.61 | 5.62 | 3.04 | 2.61 | 5.63 | 3.04 | 2.63 | 5.63 | 3.04 | 2.63 | 5.64 | 3.04 | 2.65 | 5.64 | 3.05 | 2.66 | 5.66 | 3.06 | 2.72 | 5.67 | 3.06 | 2.77 |
| Basalt | 5.85 | 3.17 | 2.70 | 5.90 | 3.19 | 2.69 | 5.92 | 3.20 | 2.70 | 5.92 | 3.20 | 2.70 | 5.92 | 3.20 | 2.71 | 5.92 | 3.20 | 2.72 | 5.92 | 3.20 | 2.73 | 5.92 | 3.20 | 2.74 | 5.93 | 3.21 | 2.80 | 5.93 | 3.21 | 2.85 |
| Diabase | 6.65 | 3.57 | 2.92 | 6.67 | 3.58 | 2.92 | 6.66 | 3.58 | 2.92 | 6.65 | 3.57 | 2.92 | 6.63 | 3.57 | 2.92 | 6.62 | 3.56 | 2.93 | 6.61 | 3.55 | 2.94 | 6.60 | 3.55 | 2.95 | 6.59 | 3.54 | 3.00 | 6.59 | 3.54 | 3.05 |
| Granite–granodiorite | 6.19 | 3.62 | 2.79 | 6.24 | 3.65 | 2.79 | 6.23 | 3.65 | 2.79 | 6.23 | 3.65 | 2.80 | 6.22 | 3.64 | 2.80 | 6.21 | 3.63 | 2.81 | 6.19 | 3.63 | 2.81 | 6.19 | 3.62 | 2.82 | 6.18 | 3.62 | 2.87 | 6.18 | 3.62 | 2.93 |
| Diorite | 6.42 | 3.63 | 2.86 | 6.48 | 3.66 | 2.86 | 6.49 | 3.67 | 2.87 | 6.49 | 3.67 | 2.87 | 6.49 | 3.67 | 2.88 | 6.48 | 3.67 | 2.89 | 6.48 | 3.66 | 2.90 | 6.48 | 3.66 | 2.91 | 6.48 | 3.66 | 2.96 | 6.48 | 3.66 | 3.02 |
| Gabbro–norite | 7.06 | 3.80 | 3.04 | 7.09 | 3.83 | 3.04 | 7.08 | 3.82 | 3.04 | 7.07 | 3.81 | 3.04 | 7.05 | 3.80 | 3.05 | 7.04 | 3.79 | 3.06 | 7.02 | 3.79 | 3.06 | 7.01 | 3.78 | 3.07 | 7.00 | 3.77 | 3.12 | 6.99 | 3.77 | 3.17 |
| Metagreywacke | 5.34 | 3.08 | 2.55 | 5.47 | 3.16 | 2.57 | 5.54 | 3.20 | 2.59 | 5.58 | 3.22 | 2.60 | 5.62 | 3.24 | 2.62 | 5.65 | 3.26 | 2.64 | 5.67 | 3.27 | 2.66 | 5.70 | 3.29 | 2.68 | 5.73 | 3.31 | 2.74 | 5.76 | 3.33 | 2.80 |
| Slate | 6.07 | 3.26 | 2.76 | 6.12 | 3.29 | 2.76 | 6.14 | 3.30 | 2.77 | 6.15 | 3.30 | 2.77 | 6.15 | 3.31 | 2.78 | 6.16 | 3.31 | 2.79 | 6.16 | 3.31 | 2.80 | 6.16 | 3.31 | 2.82 | 6.17 | 3.32 | 2.87 | 6.18 | 3.32 | 2.93 |
| Phyllite | 6.08 | 3.44 | 2.76 | 6.16 | 3.48 | 2.77 | 6.17 | 3.49 | 2.78 | 6.17 | 3.49 | 2.78 | 6.17 | 3.49 | 2.79 | 6.16 | 3.48 | 2.79 | 6.16 | 3.48 | 2.80 | 6.15 | 3.48 | 2.81 | 6.15 | 3.48 | 2.86 | 6.15 | 3.48 | 2.92 |
| Zeolite facies basalt | 6.25 | 3.36 | 2.81 | 6.32 | 3.40 | 2.82 | 6.34 | 3.41 | 2.83 | 6.35 | 3.41 | 2.83 | 6.35 | 3.41 | 2.84 | 6.35 | 3.41 | 2.85 | 6.35 | 3.41 | 2.86 | 6.35 | 3.41 | 2.87 | 6.36 | 3.42 | 2.93 | 6.36 | 3.42 | 2.98 |
| Preh–pump facies basalt | 6.25 | 3.47 | 2.81 | 6.33 | 3.51 | 2.82 | 6.35 | 3.52 | 2.83 | 6.36 | 3.53 | 2.83 | 6.37 | 3.53 | 2.85 | 6.37 | 3.53 | 2.86 | 6.37 | 3.53 | 2.87 | 6.37 | 3.53 | 2.88 | 6.38 | 3.54 | 2.93 | 6.38 | 3.54 | 2.99 |
| Greenschist basalt | 6.65 | 3.78 | 2.92 | 6.75 | 3.84 | 2.94 | 6.60 | 3.75 | 2.90 | 6.78 | 3.85 | 2.96 | 6.78 | 3.85 | 2.97 | 6.78 | 3.85 | 2.98 | 6.77 | 3.85 | 2.99 | 6.77 | 3.84 | 3.00 | 6.77 | 3.84 | 3.05 | 6.77 | 3.84 | 3.10 |
| Granite gneiss | 6.00 | 3.47 | 2.74 | 6.13 | 3.55 | 2.76 | 6.16 | 3.57 | 2.77 | 6.16 | 3.57 | 2.77 | 6.16 | 3.57 | 2.78 | 6.16 | 3.56 | 2.79 | 6.13 | 3.55 | 2.80 | 6.12 | 3.56 | 2.80 | 6.15 | 3.56 | 2.86 | 6.15 | 3.56 | 2.92 |
| Biotite (tonalite) gneiss | 6.11 | 3.50 | 2.77 | 6.19 | 3.55 | 2.78 | 6.20 | 3.55 | 2.78 | 6.21 | 3.55 | 2.79 | 6.20 | 3.55 | 2.80 | 6.20 | 3.55 | 2.80 | 6.19 | 3.55 | 2.81 | 6.19 | 3.54 | 2.82 | 6.19 | 3.54 | 2.88 | 6.19 | 3.54 | 2.93 |
| Mica quartz schist | 6.17 | 3.46 | 2.79 | 6.29 | 3.53 | 2.81 | 6.33 | 3.55 | 2.82 | 6.34 | 3.56 | 2.83 | 6.35 | 3.56 | 2.84 | 6.35 | 3.56 | 2.85 | 6.35 | 3.57 | 2.86 | 6.36 | 3.57 | 2.88 | 6.36 | 3.57 | 2.93 | 6.37 | 3.58 | 2.98 |
| Amphibolite | 6.75 | 3.83 | 2.95 | 6.84 | 3.88 | 2.97 | 6.84 | 3.88 | 2.97 | 6.83 | 3.87 | 2.97 | 6.82 | 3.87 | 2.98 | 6.80 | 3.86 | 2.98 | 6.79 | 3.85 | 2.99 | 6.78 | 3.84 | 3.00 | 6.77 | 3.84 | 3.05 | 6.77 | 3.84 | 3.10 |
| Felsic granulite | 6.32 | 3.54 | 2.83 | 6.37 | 3.57 | 2.83 | 6.37 | 3.57 | 2.83 | 6.36 | 3.56 | 2.83 | 6.35 | 3.56 | 2.84 | 6.33 | 3.55 | 2.84 | 6.32 | 3.54 | 2.85 | 6.31 | 3.54 | 2.86 | 6.31 | 3.54 | 2.91 | 6.31 | 3.53 | 2.96 |
| Paragranulite | 6.24 | 3.53 | 2.81 | 6.31 | 3.56 | 2.81 | 6.31 | 3.56 | 2.82 | 6.30 | 3.56 | 2.82 | 6.29 | 3.55 | 2.82 | 6.27 | 3.54 | 2.83 | 6.26 | 3.54 | 2.83 | 6.25 | 3.53 | 2.84 | 6.25 | 3.53 | 2.89 | 6.24 | 3.52 | 2.94 |
| Anorthositic granulite | 6.80 | 3.66 | 2.97 | 6.86 | 3.69 | 2.97 | 6.86 | 3.69 | 2.98 | 6.86 | 3.68 | 2.98 | 6.85 | 3.68 | 2.99 | 6.84 | 3.68 | 3.00 | 6.83 | 3.67 | 3.01 | 6.82 | 3.67 | 3.01 | 6.82 | 3.67 | 3.07 | 6.82 | 3.66 | 3.12 |
| Mafic granulite | 6.75 | 3.71 | 2.95 | 6.81 | 3.74 | 2.96 | 6.80 | 3.74 | 2.96 | 6.79 | 3.73 | 2.96 | 6.77 | 6.77 | 2.97 | 6.76 | 3.72 | 2.97 | 6.74 | 3.71 | 2.98 | 6.73 | 3.70 | 2.99 | 6.72 | 3.70 | 3.04 | 6.71 | 3.69 | 3.08 |
| Mafic garnet granulite | 6.98 | 3.89 | 3.02 | 7.08 | 3.94 | 3.04 | 7.09 | 3.95 | 3.04 | 7.09 | 3.94 | 3.05 | 7.08 | 3.94 | 3.06 | 7.07 | 3.93 | 3.07 | 7.06 | 3.93 | 3.07 | 7.05 | 3.92 | 3.08 | 7.05 | 3.92 | 3.13 | 7.05 | 3.92 | 3.19 |
| Mafic eclogite | 7.89 | 4.42 | 3.27 | 7.95 | 4.46 | 3.29 | 7.95 | 4.46 | 3.30 | 7.95 | 4.45 | 3.31 | 7.94 | 4.45 | 3.31 | 7.93 | 4.44 | 3.32 | 7.91 | 4.43 | 3.33 | 7.90 | 4.43 | 3.34 | 7.90 | 4.43 | 3.39 | 7.90 | 4.43 | 3.44 |
| Serpentinite | 5.26 | 2.52 | 2.53 | 5.30 | 2.54 | 2.52 | 5.31 | 2.54 | 2.52 | 5.30 | 2.54 | 2.52 | 5.30 | 2.54 | 2.53 | 5.30 | 2.54 | 2.54 | 5.30 | 2.54 | 2.55 | 5.30 | 2.54 | 2.56 | 5.31 | 2.54 | 2.61 | 5.32 | 2.55 | 2.67 |
| Quarzite | 5.90 | 3.96 | 2.71 | 5.94 | 3.98 | 2.71 | 5.93 | 3.98 | 2.71 | 5.91 | 3.96 | 2.70 | 5.89 | 3.95 | 2.70 | 5.87 | 3.94 | 2.71 | 5.85 | 3.93 | 2.71 | 5.84 | 3.92 | 2.72 | 5.83 | 3.91 | 2.77 | 5.82 | 3.91 | 2.82 |
| Calcite marble | 6.84 | 3.65 | 2.98 | 6.84 | 3.67 | 2.97 | 6.82 | 3.66 | 2.97 | 6.80 | 3.65 | 2.96 | 6.78 | 3.64 | 2.97 | 6.76 | 3.63 | 2.97 | 6.74 | 3.62 | 2.98 | 6.73 | 3.61 | 2.99 | 6.72 | 3.60 | 3.04 | 6.70 | 3.60 | 3.08 |
| Anorthosite | 6.87 | 3.59 | 2.99 | 6.91 | 3.61 | 2.99 | 6.91 | 3.61 | 2.99 | 6.90 | 3.61 | 2.99 | 6.89 | 3.60 | 3.00 | 6.88 | 3.60 | 3.01 | 6.87 | 3.59 | 3.02 | 6.86 | 3.59 | 3.03 | 6.85 | 3.58 | 3.07 | 6.85 | 3.58 | 3.13 |
| Hornblendite | 7.07 | 4.03 | 3.04 | 7.12 | 4.06 | 3.05 | 7.11 | 4.05 | 3.05 | 7.09 | 4.04 | 3.05 | 7.07 | 4.03 | 3.06 | 7.05 | 4.02 | 3.06 | 7.03 | 4.01 | 3.07 | 7.02 | 4.00 | 3.07 | 7.01 | 4.00 | 3.12 | 7.00 | 3.99 | 3.17 |

Lithologies are from Christensen and Mooney [10]. Densities are calculated from $V_p$ using a linear velocity–density relationship [10].

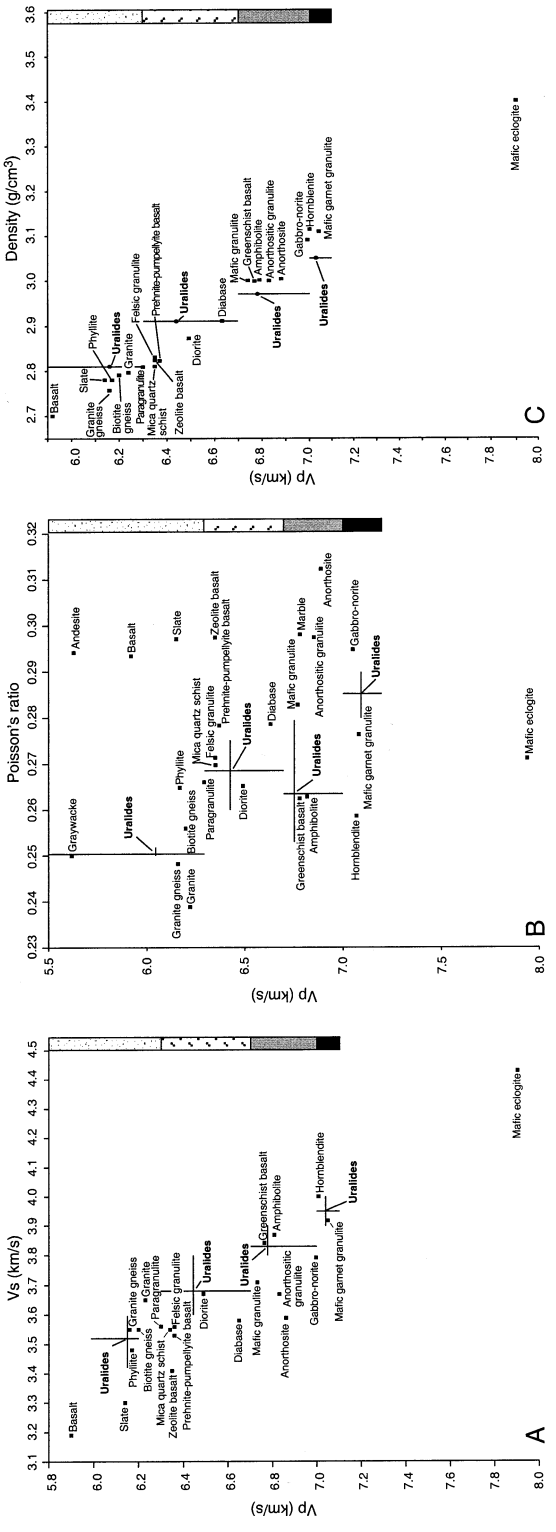


anorthosite and anorthositic granulite) (Fig. 6). The lower crust in the East Uralian zone, and the lowermost crust in the Trans-Uralian zone is best characterised by gabbro–norite, mafic garnet granulite and/or hornblendite (Fig. 6). Unfortunately, xenoliths are not found in the East Uralian zone granitoids, resulting in the absence of a key constraint on the composition of the lower crust in this area. However, recent geochemical and isotopic work on the late-orogenic granitoids in the East Uralian zone indicates that they evolved from island arc crust [47] and/or the remelting of earlier subduction-related granitoids [8] in a thickened crust. From the granitoid chemistry, it appears that the East Uralian zone may have developed as a volcanic arc built on a continental margin [8]. The melting of arc crust (whose composition is basaltic) to generate granitoids would likely result in an amphibolite (±garnet), mafic (±garnet) granulite to mafic eclogite restite being produced [48]. The physical properties of the East and Trans-Uralian zone crust do not indicate that eclogite is present, but they do suggest a middle and lower crust made up of amphibolite and/or mafic granulite, with garnet granulite, gabbro–norite, or hornblendite at the base, consistent with the petrological rationale outlined above. In contrast to the Magnitogorsk arc, intracrustal differentiation may have been active in the East and Trans-Uralian zones, with widespread melting and granitoid formation resulting in an overall granitic upper crust overlying a mafic lower crust.

One of the underlying hypotheses of the intracrustal differentiation model is that the dense res-

←

Fig. 6. (A) $V_p$ versus $V_s$ plot for the rock types listed in Table 1 and the Uralide data from Fig. 2. The horizontal and vertical lines for the Uralide data indicate the range of values (crossing at the average) in the part of the crust represented by the column on the right of the plot (see Fig. 7). (B) $V_p$ versus Poisson's ratio for the rock types listed in Table 1 and the Uralide data from Fig. 2. The Poisson's ratio value for each lithology is an average of the values listed in [9]. Horizontal and vertical lines are as in A. (C) $V_p$ versus density for the rock types listed in Table 1 and the Uralide data from Fig. 2. Densities are calculated using a linear $V_p$–density relationship for all rock types [10]. Horizontal and vertical lines are as in A.

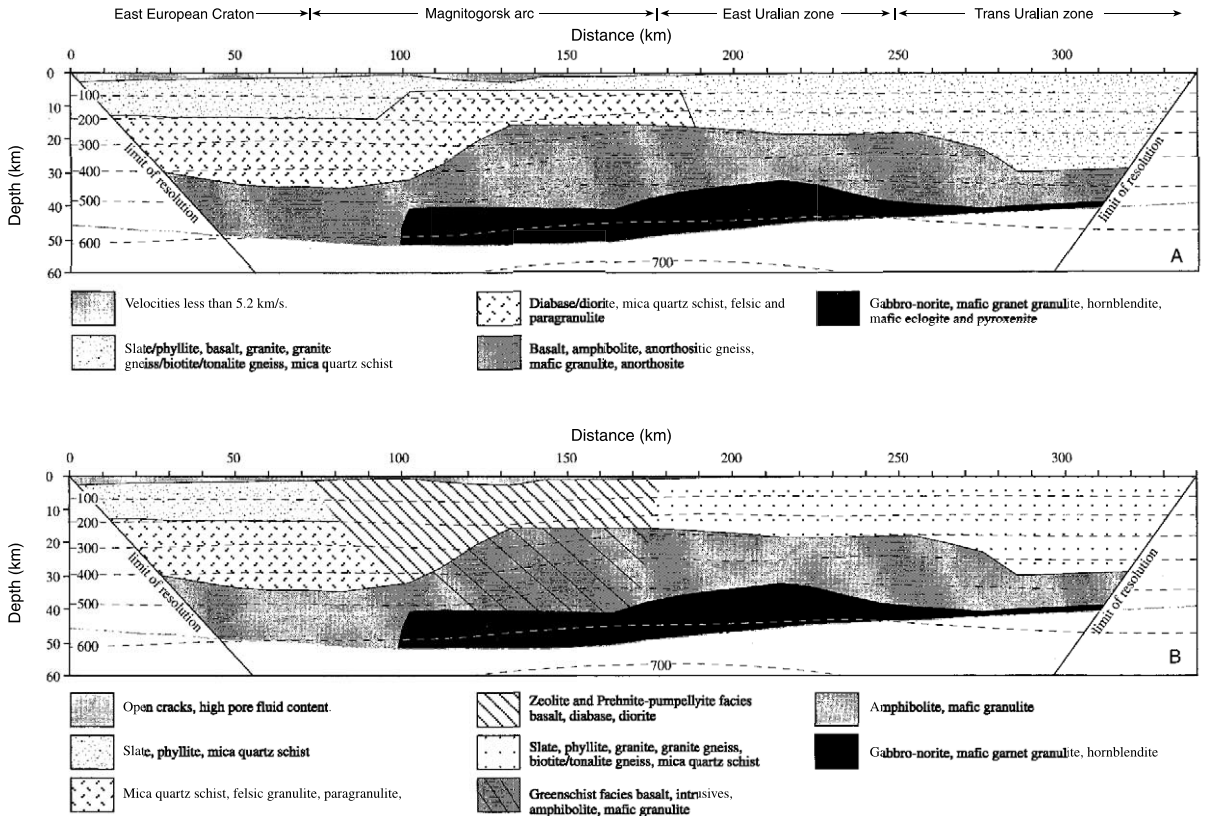


Fig. 7. (A) Model for the composition of the Uralide crust based on $V_p$, $V_s$, $\sigma$, density and magnetics. Dashed lines are geotherms in °C. (B) Model for the composition with surface geological constraints included.

tite produced by melt generation, or as the product of metamorphism, delaminates from the lower crust and together with any underlying mantle sinks into the asthenosphere [18,19,21]. Delamination (or mantle unrooting) of the lower crust and mantle has a number of consequences such as surface uplift, extension at the surface, mantle melting and intrusion into the crust, and, possibly, high-temperature metamorphism [49,50]. With the exception of the East Uralian zone, which is within a large wrench fault system, the southern Uralides show very little Palaeozoic metamorphism. This, combined with evidence from fission track data [51,52], indicates that there was very little surface uplift and erosion in the southern Uralides. Furthermore, late- and/or post-orogenic extension appears not to have taken place in the southern Uralides [30]. The late orogenic granitoids in the southern Uralides are thought to have been derived from melting of arc crust by radiogenic heat production with little, if any, input from the mantle.

Finally, post-orogenic processes, such as cooling of the Uralide lithosphere since the Palaeozoic, may also have had an important effect on the physical properties of the Uralide crust, and hence its apparent composition. Although it is thought that the lower continental crust is in granulite facies [10,11], the temperature conditions that prevail in the Uralide lower crust are well below those of granulite facies (Fig. 4D). This suggests that if granulites do occur in the Uralide lower crust, they are currently metastable and may, therefore, have undergone some change since their formation during the Uralide orogeny. It is likely that the Palaeozoic orogenic geotherm in the southern Uralides was much higher than it is today, and since apatite fission track data suggest

that the southern Uralides have undergone only minor exhumation since the Late Permian in the case of the Magnitogorsk arc and the Late Triassic in the case of the East Uralian zone [51,52], it can perhaps be assumed that the Uralide crust has undergone near-isobaric cooling since the end of the orogeny. Furthermore, the good quality of the S-wave arrivals in the horizontal component of the geophones in the URSEIS wide-angle experiment indicates that there is very little attenuation for the S-waves [34], suggesting that the Uralide crust contains little, if any, fluid at present. In fluid-absent conditions, isobaric cooling might preserve granulite [53], while leading to reactions that result in an increase in the percentage of garnet [12], which would lead to an increase in seismic velocities and density [10]. If fluid was present with a water activity high enough to destabilise anhydrous mineral assemblages, the granulite would have been (in part or in whole) retrogressed to amphibolite [53], whose physical properties cannot be differentiated from those of mafic granulite in this dataset.

## 5. Conclusions

$V_p$, $V_s$, $\sigma$, heat flow, gravity and magnetic data suggest an array of possible crustal compositions in a variety of metamorphic facies along the transect, but by incorporating the surface geology and correcting the laboratory velocity measurements for the Uralide temperature/depth function, tighter constraints can be placed on the interpretation. The interpretation does not take into account the effect that finely layered mixtures of rock types would have on the physical properties presented for the Uralides, nor are eclogite facies rocks other than mafic eclogite considered. Nevertheless, the Uralide crust along the URSEIS transect appears to have a more complex composition than that suggested by a simplified two-layer continental crustal composition model of a granitic upper crust overlying a more mafic lower crust. Although this two-layer model is true in general for the Uralides there are clear differences between the composition of the old continental crustal nucleus of the East European Craton and the newly added crust of the accreted arc terranes to the east. These arc terranes also display internal differences. In particular, the middle crust of the East European Craton is more felsic than that of the Magnitogorsk and East Uralian zones, and the latter two have a lowermost crust whose characteristics possibly indicate a higher garnet content and/or the presence of hornblendite (see also [54]). The composition of the easternmost part of the Trans-Uralian zone middle crust is significantly less mafic than that of the arc terranes to the west. It is clear from the physical properties that eclogite does not exist in the lower crust along the URSEIS transect. The absence of eclogite in the Uralide lower crust, particularly in the arc terranes, may be taken as evidence for the intracrustal differentiation model in which the eclogite has delaminated and sunk into the mantle. However, there is very little evidence, such as surface uplift, metamorphism or the petrologial signature of the granitoids, to suggest that crustal thinning occurred on a large enough scale to have affected the bulk composition of the Uralide crust in this way. Cooling of the Uralide crust from its orogenic to its present thermal condition may have had a significant effect on its physical properties, caused in particular by the amount of garnet and amphibole present in the mafic middle and lower crust. However, because of the similar physical properties of mafic garnet granulite and hornblendite it is not possible to differentiate between these two rock types.

## Acknowledgements

This project was funded by BTE2002-04618-C02-02/. M. Fernandez, C. Juhlin, H. Austrheim, J. Gallart and J. Alvarez-Marron are thanked for reviews of earlier drafts of the manuscript. Journal reviewers W. Mooney and S. Smithson are also thanked. ***[SK]***

## References

[1] R.L. Rudnick, Making continental crust, Nature 378 (1995) 571–578.

[2] A.M.C. Sengor, B.A. Natal'in, V.S. Burtman, Evolution of the Altaid tectonic collage and Paleozoic crustal growth in Eurasia, Nature 364 (1993) 299–307.
[3] A.M. Sengor, B.A. Natal'in, Turkic-type orogeny and its role in the making of the continental crust, Annu. Rev. Earth Planet. Sci. 24 (1996) 263–337.
[4] V.N. Puchkov, Structure and geodynamics of the Uralian orogen, in: J.-P. Burg, M. Ford (Eds.), Orogeny Through Time, Geol. Soc. Spec. Publ. 121 (1997) 201–236..
[5] D. Brown, C. Juhlin, J. Alvarez-Marron, A. Perez-Estaun, A. Oslianski, Crustal-scale structure and evolution of an arc-continent collision zone in the southern Urals, Russia, Tectonics 17 (1998) 158–171.
[6] D. Brown, P. Spadea, Processes of forearc and accretionary complex formation during arc-continent collision in the southern Ural Mountains, Geology 27 (1999) 649–652.
[7] M. Friberg, C. Juhlin, M. Beckholmen, G.A. Petrov, A.G. Green, Palaeozoic tectonic evolution of the Middle Urals in the light of the ESRU seismic experiments, J. Geol. Soc. London 159 (2002) 295–306.
[8] F. Bea, G.B. Fershtater, P. Montero, Granitoids on the Uralides: Implications for the evolution of the orogen, in: D. Brown, C. Juhlin, V. Puchkov (Eds.) Mountian Building in the Uralides: Pangea to Present, AGU Geophys. Monogr. Ser., 2002.
[9] N.I. Christensen, Poisson's ratio and crustal seismology, J. Geophys. Res. 101 (1996) 3139–3156.
[10] N.I. Christensen, W.D. Mooney, Seismic velocity structure and composition of the continental crust: A global view, J. Geophys. Res. 100 (1995) 9761–9788.
[11] R.L. Rudnick, D.M. Fountain, Nature and composition of the continental crust: A lower crustal perspective, Rev. Geophys. 33 (1995) 267–309.
[12] S.L. Harley, The origins of granulites: A metamorphic perspective, Geol. Mag. 126 (1989) 215–247.
[13] J.A. Percival, D.M. Fountain, M.H. Salisbury, Exposed crustal cross sections as windows on the lower crust, in: D.M. Fountain, R. Arculus, R.W. Kay (Eds.), Continental Lower Crust, Elsevier, New York, 1992, pp. 317–362.
[14] R.L. Rudnick, Xenoliths – Samples of the lower continental crust, in: D.M. Fountain, R. Arculus, R.W. Kay (Eds.), Continental Lower Crust, Elsevier, New York, 1992, pp. 269–308.
[15] S.R. Taylor, S.M. McLennan, The composition and evolution of the continental crust: Rare earth element evidence from sedimentar rocks, Phil. Trans. R. Soc. London 301 (1995) 381–399.
[16] W.S. Holbrook, W.D. Mooney, N.I. Christensen, The seismic velocity structure of the deep continental crust, in: D.M. Fountain, R. Arculus, R.W. Kay (Eds.), Continental Lower Crust, Elsevier, New York, 1992, pp.
[17] R.J. Arculus, Aspects of magma genesis in arcs, Lithos 33 (1994) 189–208.
[18] N.T. Arndt, S.L. Goldstein, An open boundary between lower continental crust and mantle: Its role in crust formation and crustal recycling, Tectonophysics 161 (1989) 201–212.
[19] R.W. Kay, S. Mahlburg-Kay, Creation and destruction of the lower continental crust, Geol. Rundsch. 80 (1991) 259–278.
[20] H. Austrheim, Eclogite formation and dynamics of crustal roots under continental collision zones, Terra Nova 3 (1991) 492–499.
[21] M.A. Kamaletdinov, The Nappe Structures of the Urals (in Russian), Nauka, Moscow, 1974, 228 pp.
[22] D. Brown, J. Alvarez-Marron, A. Perez-Estaun, Y. Gorozhanina, V. Baryshev, V. Puchkov, Geometric and kinematic evolution of the foreland thrust and fold belt in the southern Urals, Tectonics 16 (1997) 551–562.
[23] A. Perez-Estaun, J. Alvarez-Marron, D. Brown, V. Puchkov, Y. Gorozhanina, V. Baryshev, Along-strike structural variations in the foreland thrust and fold belt of the southern Urals, Tectonophysics 276 (1997) 265–280.
[24] A.V. Maslov, B.D. Erdtmann, K.S. Ivanov, S.N. Ivanov, M.T. Krupenin, The main tectonic events, depositional history, and the palaeogeography of the southern Urals during the Riphean–early Paleozoic, Tectonophysics 276 (1997) 313–335.
[25] B.I. Chuvashov, V.A. Chermynkh, V.V. Chernykh, V.J. Kipin, V.A. Molin, V.P. Ozhgibesov, P.A. Sofronitsky, The Permian system: Guides to geological excursions in the Uralian type localities, part 2 – southern Urals. Occas. Publ. ESRI N. Ser. 10, (1993) 303 pp.
[26] J. Alvarez-Marron, D. Brown, A. Perez-Estaun, V. Puchkov, Y. Gorozhanina, Accretionary complex structure and kinematics during Paleozoic arc–continent collision in the southern Urals, Tectonophysics 324 (2000) 175–191.
[27] V.A. Maslov, V.L. Cherkasov, V.T. Tischchenko, A.I. Smirnova, O.V. Artyushkova, V.V. Pavlov, On the Stratigraphy and Correlation of the Middle Paleozoic Complexes of the Main Copper-pyritic Areas of the Southern Urals (in Russian), Ufimsky Nauchno-Issled. Tsentr, Ufa, 1993.
[28] D. Brown, J. Alvarez-Marron, A. Perez-Estaun, V. Puchkov, Y. Gorozhanina, P. Ayarza, Structure and evolution of the Magnitogorsk forearc basin: Identifying into upper crustal processes during arc-continent collision in the southern Urals, Tectonics 20 (2001) 364–375.
[29] V.N. Puchkov, Paleogeodynamics of the Central and Southern Urals (in Russian), Ufa Pauria, 2000, 145 pp.
[30] A. Tryggvason, D. Brown, A. Perez-Estaun, Crustal structure of the southern Uralides from true amplitude processing of the Urals Seismic Experiment and Integrated Studies (URSEIS) vibroseis profile, Tectonics 20 (2001) 1040–1052.
[31] D. Brown, C. Juhlin, A. Tryggvason, D. Steer, P. Ayarza, M. Beckholmen, A. Rybalka, M. Bliznetsov, The crustal architecture of the southern and middle Urals from the URSEIS, ESRU, and Alapaev reflection seismic profiles, in: D. Brown, C. Juhlin, V. Puchkov (Eds.) Mountian

Building in the Uralides: Pangea to Present, AGU Geophys. Monogr. Ser., 2002.
[32] D.N. Steer, J.H. Knapp, L.D. Brown, H.P. Echtler, D.L. Brown, R. Berzin, Deep structure of the continental lithosphere in an unextended orogen: An explosive-source seismic reflection profile in the Urals (Urals Seismic Experiment and Integrated Studies (URSEIS 1995)), Tectonics 17 (1998) 143–157.
[33] R. Carbonell, D. Lecerf, M. Itzin, J. Gallart, D. Brown, Mapping the Moho beneath the southern Urals, Geophys. Res. Lett. 25 (1998) 4229–4233.
[34] R. Carbonell, J. Gallart, A. Perez-Estaun, J. Diaz, S. Kashubin, J. Mechie, F. Wenzel, J. Knapp, Seismic wide-angle constraints on the crust of the southern Urals, J. Geophys. Res. 105 (2000) 13755–13777.
[35] R. Carbonell, M.A. Speece, W.P. Clement, S.B. Smithson, Anisotropy measurements and the deep structure of a passive margin: Southwestern Greenland, in: E. Banda, M. Torne, M. Talwani (Eds.), Ocean Continent Boundaries, NATO ASI Series, vol. 463, Kluwer, Dordrecht, 1995, pp. 121–146.
[36] I.T. Kukkonen, I.V. Golovanova, Y. Khachay, V.S. Druzhinin, A.M. Kosarev, V.A. Schapov, Low geothermal heat flow of the Urals fold belt - Implication of low heat production, fluid circulation or palaeoclimate, Tectonophysics 276 (1997) 63–86.
[37] I.T. Kukkonen, J. Jokinen, U. Seipold, Temperature and pressure dependencies of thermal transport properties of rocks: Implications for uncertainties in thermal lithosphere models and new laboratory measurements of high-grade rocks in the Central Fennoscandian Shield, Surv. Geophys. 20 (1999) 33–59.
[38] G.S. Kimbell, C. Ayala, A. Gerdes, M.K. Kaban, V.A. Shapiro, Y.P. Menshikov, Insights into the architecture and evolution of the southern and middle Urals from gravity and magnetic data, in: D. Brown, C. Juhlin, V. Puchkov (Eds.) Mountian Building in the Uralides: Pangea to Present, AGU Geophys. Monogr. Ser., 2002.
[39] C. Ayala, G.S. Kimbell, D. Brown, P. Ayarza, Y.P. Menshikov, Magnetic evidence for the geometry and evolution of the eastern margin of the East European Craton in the southern Urals, Tectonophysics 320 (2000) 31–44.
[40] S.V. Sobolov, A.Yu. Babeyko, Modeling of mineralogical composition, density and elastic wave velocities in anhydrous magmatic rocks, Surv. Geophys. 15 (1994) 515–544.
[41] C.C. Diaconescu, J.H. Knapp, Role of a phase-change Moho in stabilization and preservation of the southern Uralide orogen, Russia, in: D. Brown, C. Juhlin, V. Puchkov (Eds.), Mountian Building in the Uralides: Pangea to Present, AGU Geophys. Monogr. Ser., 2002.
[42] R. Carbonell, J. Gallart, A. Perez-Estaun, Modelling and imaging the Moho transition: The case of the southern Urals, Geophys. J. Int. 148 (2002) 1–15.
[43] M.M. Fliedner, S.L. Klemperer, Structure of an island arc: Wide-angle seismic studies in the eastern Aleutian islands, Alaska, J. Geophys. Res. 104 (1999) 10667–10694.
[44] W.S. Holbrook, D. Lizarralde, S. McGeary, N. Bangs, J. Diebold, Structure and composition of the Aleutian island arc and implications for continental crustal growth, Geology 27 (1999) 31–34.
[45] D.J. Miller, N.I. Christensen, Seismic signature and geochemistry of an island arc: A multidisiplinary study of the Kohistan accreted terrane, northern Pakistan, J. Geophys. Res. 99 (1994) 11623–11642.
[46] P. Spadea, M. D'Antonio, A. Kosarev, Y. Gorozhanina, D. Brown, Arc–continent collision in the southern Urals: Petrogenetic aspects of the fore-arc complex, in: D. Brown, C. Juhlin, V. Puchkov (Eds.) Mountian Building in the Uralides: Pangea to Present, AGU Geophys. Monogr. Ser., 2002.
[47] A. Gerdes, P. Montero, F. Bea, G. Fershtater, N. Borodina, T. Osipova, G. Shardakova, Int. J. Earth Sci. 9 (2002) 1–17.
[48] R.P. Rapp, E.B. Watson, Dehydration melting of metabasalt at 8–32 kbar: Implication for continental growth and crust-mantle recycling, J. Petrol. 36 (1995) 891–931.
[49] J.P. Platt, P.C. England, Convective removal of lithosphere beneath mountain belts: Thermal and mechanical consequences, Am. J. Sci. 293 (1993) 307–336.
[50] A.M. Marotta, M. Fernandez, R. Sabadini, Mantle unrooting in collisional settings, Tectonophysics 296 (1998) 31–46.
[51] D. Seward, A. Perez-Estaun, V. Puchkov, Preliminary fission-track results from the southern Urals – Sterlitamak to Magnitogorsk, Tectonophysics 276 (1997) 281–290.
[52] D. Seward, D. Brown, R. Hetzel, M. Friberg, A. Gerdes, G.A. Petrov, A. Perez-Estaun, The syn- and post-orogenic low temperature events in the southern and middle Urals: Evidence from fission-track analysis, in: D. Brown, C. Juhlin, V. Puchkov (Eds.) Mountian Building in the Uralides: Pangea to Present, AGU Geophys. Monogr. Ser., 2002.
[53] H. Austrheim, Influence of fluid and deformation on metamorphism of the deep crust and consequences for the geodynamics of collisions zones, in: B.R. Hacker, J.G. Liou (Eds.) When Continents Collide: Geodynamics and Geochemistry of Ultrahigh-Pressure Rocks, Kluwer, Amsterdam, 1998, pp. 297–323.
[54] J. Scarrow, C. Ayala, G.S. Kimbell, Insights into orogensis: getting to the root of the continent – ocean–continent collision in the southern Urals, Russia, J. Geol. Soc. 159 (2002) 659–672.